# Fine and hyperfine interactions in cold YbF-He collisions in electromagnetic fields

T. V. Tscherbul,[1,*] J. Kłos,[2] L. Rajchel,[3,4] and R. V. Krems[1]
[1]*Department of Chemistry, University of British Columbia, Vancouver, B.C., Canada V6T 1Z1*
[2]*Department of Chemistry and Biochemistry, University of Maryland, College Park, Maryland 20742-2021, USA*
[3]*Department of Chemistry, Oakland University, Rochester, Michigan 48309, USA*
[4]*Faculty of Chemistry, Warsaw University, Pasteura 1, 03-093 Warszawa, Poland*
(Received 26 December 2006; published 26 March 2007)

We present a rigorous study of cold and ultracold collisions of YbF($^2\Sigma$) molecules with He atoms in external electric and magnetic fields based on an accurate calculation of the interaction potential surface and quantum theory of atom-molecule scattering. We analyze the mechanisms of collisional depolarization of the electron and nuclear spins of YbF and demonstrate that the rate constants for elastic and inelastic collisions of YbF with He are sensitive to the magnitudes of the applied fields. Collisions of heavy polar molecules like YbF may thus be easily manipulated with external electromagnetic fields. We show that collisional spin relaxation of YbF molecules in rotationally excited states is suppressed by electric fields much more significantly than the spin relaxation in the ground rotational state. We explain this by the influence of electric-field-induced Feshbach resonances, which occur at much lower collision energies when the molecule is rotationally excited. Our results suggest that heavy polar molecules may be amenable to magnetic trapping in a buffer gas of He, which could greatly enhance the sensitivity of spectroscopic experiments to measure the electric dipole moment of the electron.

DOI: 10.1103/PhysRevA.75.033416 PACS number(s): 33.80.Ps, 34.50.Pi

## I. INTRODUCTION

A major goal of several recent experiments has been to measure the electric dipole moment (EDM) of the electron [1–5]. A nonzero value of the EDM would indicate violation of the time-reversal symmetry of nature and inadequacy of the standard model of elementary particles [1,2,6]. Several authors proposed to analyze the electric properties of the electron based on precision spectroscopy measurements of molecular energy levels. The electrons in molecules are subjected to extremely high electric fields and polarization of molecules in an external field may lead to energy shifts dependent on the EDM of the electron. For example, Hinds and co-workers [3] applied electric fields to orient YbF($^2\Sigma$) molecules and measure the differential Stark shift between two magnetic sublevels of the $F=1$ hyperfine state using molecular interferometry. The sensitivity of the measurements can be greatly enhanced if the molecules are cooled to below 20 K, which increases the population of the ground rotational level and leads to longer observation times. Cold beams of YbF molecules have been recently produced by Stark deceleration [7] and experiments are planned to generate a cold beam of YbF using buffer gas cooling in helium as demonstrated in Ref. [8]. Egorov *et al.* proposed to carry out EDM measurements with PbO molecules directly in the buffer gas of helium [5]. Collisions with helium atoms may, however, destroy the coherent superpositions of hyperfine sublevels by inducing hyperfine relaxation and electron spin changing transitions. It is therefore important to understand the mechanisms of collisionally induced electron spin and nuclear spin depolarization of heavy polar molecules like YbF.

Buffer gas loading of molecules in a magnetic trap is one of the most general techniques for the creation of cold molecules [9]. The efficiency of magnetic trapping of molecules is, however, limited by collisional spin relaxation in helium. Theoretical studies of Krems *et al.* [10] showed that molecules in the $^2\Sigma$ electronic state are generally most immune to collisional spin relaxation and indicated that spin relaxation rates in light $^2\Sigma$ molecules can be scaled as $\gamma^2/B_e^n$, where $\gamma$ is the spin-rotation interaction constant, $B_e$ is the rotational constant of the molecule and $n>1$. These results suggested that magnetic trapping of heavy $^2\Sigma$ molecules like YbF should be very difficult due to fast spin relaxation although no rigorous calculations for molecules with small rotational constants have been reported to support this argument. In addition, the mechanism of spin relaxation of heavy $^2\Sigma$ molecules may be modified by strong hyperfine interactions not considered previously [10,12]. The hyperfine constant of YbF is 141.8 MHz, 10 times larger than the spin-rotation interaction constant 13.4 MHz [13]. The hyperfine interaction couples the electron and nuclear spins and may induce spin relaxation. Maussang *et al.* [11] have recently observed significant rates of spin relaxation in collisions of CaF($^2\Sigma$) molecules with He atoms, which could result from the hyperfine coupling of the spin levels.

The methodology to describe collision-induced hyperfine transitions was developed by Alexander and Dagdigian [14] for the study of collisions of $^2\Sigma$ molecules with structureless atoms. Their theory was subsequently used for the analysis of more complex molecules such as $N_2H^+$ and HCN in the interstellar space [15,16]. Bohn *et al.* included hyperfine interactions in their studies of cold collisions of OH($^2\Pi$) radicals in electric [17,18] and magnetic [19] fields. Very recently, Lara *et al.* calculated cross sections for inelastic transitions in cold Rb-OH collisions relevant for sympathetic cooling experiments and found hyperfine interactions to be important [20]. However, no dynamical calculations for heavy polar molecules with strong hyperfine interactions in superimposed electric and magnetic fields have been reported.

*Electronic address: timur@chem.ubc.ca

 

In this work, we calculate the interaction potential between YbF($^2\Sigma$) molecules and He and extend the work of Alexander and Dagdigian to study the role of fine and hyperfine interactions in collisions of YbF($^2\Sigma$) molecules with He atoms in the presence of superimposed electric and magnetic fields. We find new mechanisms of spin relaxation determined by the interplay of hyperfine and spin-rotation interactions and the interactions induced by external fields. Our results suggest that hyperfine interactions are important and demonstrate that the dynamics of heavy polar molecules at $T \sim 0.1$ K can be effectively manipulated by superimposed electric and magnetic fields. We demonstrate that the orientation of cold molecules with electric fields leads to electric-field induced Feshbach resonances.

## II. THEORY

### A. Potential energy surface for YbF-He

The electronic structure of YbF in the ground electronic state $^2\Sigma$ is determined predominantly by the ionic configuration $f^{14}6s^1$(Yb)-$2p_z$(F). We used the MOLPRO 2002.6 suite of programs [21] to calculate the interaction potential between YbF and He. Our approach is based on the supermolecular method using dimer centered basis set for monomer fragments and the procedure of Boys and Bernardi to correct for the basis set superposition error [22]. The interaction energy is calculated as the difference between the total energy of YbF-He and the sum of the total energies of isolated YbF and He. The potential energy surface (PES) is constructed in the Jacobi coordinates $r, R, \theta$, where $\theta=0$ corresponds to the YbF-He collinear arrangement. Assuming the rigid rotor approximation, we fixed the distance of YbF at the equilibrium value $r=3.853a_0$. The radial grid covered the repulsive wall from $3.0a_0$ to the long range distance $24.0a_0$ with 44 grid points. The angular grid consisted of 12 points: $\theta \in [0, 11.25, 22.5, 33.75, 45, 56.25, 67.5, 90, 112.5, 135, 157.5, 180]$ degrees.

We employed the basis set $(14s, 13p, 10d, 8f, 6g)$ for Yb contracted to $[6s, 6p, 5d, 4f, 3g]$ of Dolg *et al.* [23] with the effective core potential of 28 core electrons. The basis was augmented by one $p$ and one $d$ diffuse functions with the exponents 0.028 and 0.032, respectively, as described by Buchachenko *et al.* [24]. For the fluorine atom we used an augmented, correlation consistent triple-zeta basis set (aug-cc-pvtz) of Dunning *et al.* [25] supplemented with additional $s$, $p$, and $d$ diffuse functions with the exponents 0.0276, 0.0203, and 0.0997 to achieve a better description of the anionic character of F in the YbF molecule. The final basis set comprised 451 primitive functions. The helium atom was described by the aug-cc-pvqz basis set of Dunning *et al.* To describe the van der Waals interaction more accurately, we included an additional set of $3s3p2d$ midbond functions. Using canonicalized orbitals from a complete active space self-consisted-field (CASSCF) calculation with 21 electrons in 11 active orbitals, we performed restricted Hartree-Fock (RHF) calculations for the $^2\Sigma$ state of YbF interacting with He. The initial CASSCF calculation was to ensure that we obtain proper symmetry wave functions for the YbF($^2\Sigma$)-He dimer and for the YbF($^2\Sigma$) molecule. The RHF wave functions were then used in the partially spin restricted coupled cluster with single, double, and noniterative triple excitations [RCCSD(T)] calculations.

To obtain an analytical representation of the potential energy surface for YbF-He we approximated the calculated points by the expression given in Ref. [26] including 10 long range van der Waals coefficients from $C_{6,0}$ to $C_{9,5}$. The final root mean square error of the fit was 26 cm$^{-1}$. The largest contributions to this error come from the repulsive region on the side of the fluorine atom. The residual errors in the vicinity of the global minimum are on the order of 0.06 cm$^{-1}$ which is 0.3% of the absolute magnitude of the potential. A table of interaction energies and the Fortran programs generating the potential energy surface are available from the authors upon request.

### B. Dynamical calculations

The total Hamiltonian of the YbF-He complex in an external electromagnetic field can be written as

$$\hat{H} = -\frac{1}{2\mu R}\frac{d^2}{dR^2}R + \frac{\hat{\ell}^2(\theta_R, \phi_R)}{2\mu R^2} + \hat{V}(r, R, \theta) + \hat{H}_{\mathrm{mol}}(r, \theta_r, \phi_r), \tag{1}$$

where $R$ is the center-of-mass separation between the atom and the molecule, $\theta_R$, $\phi_R$ specify the orientation of the atom-molecule separation vector in a space-fixed coordinate frame, $r$, $\theta_r$, $\phi_r$ are the coordinates of the vector joining the nuclei of YbF, $\theta$ is the Jacobi angle of the YbF-He complex, $\mu$ is the reduced mass of the complex, $\hat{\ell}$ is the orbital angular momentum for the relative motion of YbF and He and $\hat{V}(r, R, \theta)$ is the atom-molecule interaction potential. The diatomic molecule is described by the Hamiltonian

$$\hat{H}_{\mathrm{mol}}(r, \theta_r, \phi_r) = B_e\hat{N}^2 + \gamma\hat{N}\cdot\hat{S} + \hat{V}_{\mathrm{Zeeman}} + \hat{V}_{\mathrm{Stark}} + \hat{V}_{\mathrm{hf}}, \tag{2}$$

where $B_e$ is the rotational constant, $\hat{N}$ is the rotational angular momentum, $\hat{S}$ is the electron spin, and $\gamma$ is the spin-rotation interaction constant. In Eq. (2), we have neglected the $P$- and $P$, $T$-odd interactions [1,30,31]. These perturbations are known to be extremely weak and, albeit important for EDM search experiments [30,31], are unlikely to alter collisional dynamics of YbF at cold temperatures $\sim 0.1$ K of interest for the present work. If the magnetic field $\hat{B}$ is directed along the space-fixed $Z$ axis, the interaction with magnetic fields takes the form $\hat{V}_{\mathrm{Zeeman}} = 2\mu_B B\hat{S}_Z$, where $\mu_B$ is the Bohr magneton, and the operator $\hat{S}_Z$ stands for the projection of the electron spin. The interaction with an electric field can be written as $\hat{V}_{\mathrm{Stark}} = -dE\cos\chi$, where $d$ is the molecular dipole moment, $E$ is the electric field strength, and $\chi$ is the angle between the molecular axis and the field direction. The projection of the total angular momentum is not conserved and the calculations are prohibitively difficult if the electric and magnetic fields are not parallel. Changing the relative

orientation of magnetic and electric fields may affect the magnitude of the scattering cross sections near avoided crossings [32] but should leave the qualitative picture unchanged. Here, we will assume that the electric field is parallel to the magnetic field.

The hyperfine structure of $^{174}$Yb$^{19}$F arises from the spin $I=1/2$ of the F nucleus and it is described by the operator

$$\hat{V}_{\rm hf} = (b+c/3)\hat{I}\cdot\hat{S} + \frac{c\sqrt{6}}{3}\left(\frac{4\pi}{5}\right)^{1/2} \times \sum_{q=-2}^{2} (-1)^q Y_{2-q}(\theta_r,\phi_r)[\hat{I}\otimes\hat{S}]_q^{(2)} + C\hat{I}\cdot\hat{N}, \quad (3)$$

where $Y_{2-q}(\theta_r,\phi_r)$ is a spherical harmonic. The first term in this expression is similar to the spin-rotation interaction, while the second term has the same form as the spin-spin interaction in $^3\Sigma$ molecules. The nuclear spin-rotation interaction constant $C=6.8\times10^{-7}$ cm$^{-1}$ is $\sim10^3$ times smaller than the constants $b$ and $c$ [13]. We therefore neglect this interaction.

The collision problem in the presence of time-independent external fields is most easily described by the close coupling method based on the expansion of the eigenfunction of the total Hamiltonian in a fully uncoupled basis [10]

$$|NM_N\rangle|SM_S\rangle|IM_I\rangle|\ell M_\ell\rangle, \quad (4)$$

where the projections of all angular momenta are taken with respect to the field direction. The total wave function of the system can be expanded as

$$\Psi^M = \frac{1}{R}\sum_{\ell,M_\ell}\sum_{N,M_N}\sum_{M_S}\sum_{M_I} F^M_{NM_NM_SM_I\ell M_\ell}(R)|NM_N\rangle|SM_S\rangle|IM_I\rangle \times|\ell M_\ell\rangle, \quad (5)$$

where the expansion coefficients $F^M_{NM_NM_SM_I\ell M_\ell}(R)$ depend on the radial coordinate. The total electron and nuclear spins $S$ and $I$ are conserved. Electric and magnetic fields couple different total angular momentum states, but the projection $M=M_N+M_S+M_I+M_\ell$ of the total angular momentum on the field axis is a good quantum number in parallel fields. The substitution of the expansion (5) in the Schrödinger equation yields a system of coupled differential equations

$$\left(\frac{d^2}{dR^2}+2\mu E_{\rm tot}-\frac{\ell(\ell+1)}{R^2}\right)F^M_{NM_NM_SM_I\ell M_\ell}(R) = 2\mu\sum_{N',M_N'}\sum_{M_S',M_I'}\sum_{\ell',M_\ell'}\langle NM_N|\langle SM_S|\langle IM_I|\langle\ell M_\ell|\hat{V}(R,r,\theta) + \hat{H}_{\rm mol}|N'M_N'\rangle|SM_S'\rangle|IM_I'\rangle|\ell'M_\ell'\rangle F^M_{N'M_N'M_S'M_I'\ell'M_\ell'}(R), \quad (6)$$

where $E_{\rm tot}$ is the total energy. The explicit expressions for the matrix elements of the spin-rotation interaction and the atom-molecule interaction potential were given in Ref. [10] and the matrix elements of the Stark interaction were evaluated in Refs. [17,18,27]. The matrices of the centrifugal and Zeeman interactions in the uncoupled basis (4) are diagonal. The matrix elements of the hyperfine interaction can be evaluated using the Wigner-Eckart theorem [28]. For the first hyperfine term $(b+c/3)\hat{I}\cdot\hat{S}$, we have

$$\langle NM_N|SM_S|IM_I|\ell M_\ell|(b+c/3)\hat{I}\cdot\hat{S}|N'M_N'|SM_S'|IM_I'|\ell'M_\ell'\rangle = \delta_{NN'}\delta_{\ell\ell'}\delta_{M_\ell M_\ell'}\delta_{M_NM_N'}\Big[(b+c/3)\,\delta_{M_IM_I'}\delta_{M_SM_S'}M_IM_S + \left(\frac{b+c/3}{2}\right)\delta_{M_IM_I'\pm1}\delta_{M_SM_S'\mp1} \times[I(I+1)-M_I'(M_I'\pm1)]^{1/2} \times[S(S+1)-M_S'(M_S'\mp1)]^{1/2}\Big]. \quad (7)$$

The matrix elements of the second term of the hyperfine interaction (3) are

$$\langle NM_N|SM_S|IM_I|\ell M_\ell\left|\frac{c\sqrt{6}}{3}\left(\frac{4\pi}{5}\right)^{1/2}\sum_{q=-2}^{2}(-1)^qY_{2-q}(\theta_r,\phi_r)[\hat{I}\otimes\hat{S}]_q^{(2)}\right|N'M_N'|SM_S'|IM_I'|\ell'M_\ell'\rangle = \delta_{\ell\ell'}\delta_{M_\ell M_\ell'}\frac{c\sqrt{30}}{30}[(2S+1)S(S+1)]^{1/2}[(2I+1)I(I+1)]^{1/2}[(2N+1)(2N'+1)]^{1/2}(-1)^{S+I-M_F} \times\begin{pmatrix}N & 2 & N'\\ -M_N & -q_N & M_N'\end{pmatrix}\begin{pmatrix}N & 2 & N'\\ 0 & 0 & 0\end{pmatrix}\begin{pmatrix}1 & 1 & 2\\ q_S & q_I & -q_N\end{pmatrix}\begin{pmatrix}S & 1 & S\\ -M_S & q_S & M_S'\end{pmatrix}\begin{pmatrix}I & 1 & I\\ -M_I & q_I & M_I'\end{pmatrix}, \quad (8)$$

where $q_N=M_N'-M_N$, $q_S=M_S-M_S'$, $q_I=M_I-M_I'$. The projection of the total angular momentum of the diatomic molecule is given by $M_F=M_N+M_S+M_I$. The third $3j$ symbol in Eq. (8) is nonzero only when $q_N=q_S+q_I$, which ensures that the total angular momentum projection $M_F$ of the molecule is conserved [29].

We used the following spectroscopic constants for $^{174}$Yb$^{19}$F [13] (in units of cm$^{-1}$): $B_e=0.241\,29$, $\gamma=4.4778$

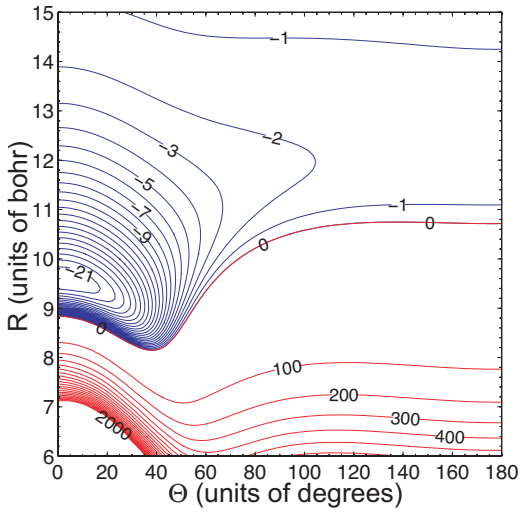


FIG. 1. (Color online) Contour map of the calculated PES for YbF-He. $\theta=0$ corresponds to the He-FYb arrangement.

$\times 10^{-4}$, $b=4.729\,83\times 10^{-3}$, $c=2.848\,75\times 10^{-3}$. The dipole moment of YbF is $d=3.914$ D [13]. The rotational states $|NM_N\rangle$ up to $N=8$ and partial waves $|\ell M_\ell\rangle$ up to $\ell=8$ were included in the basis set (4) to ensure convergence of the cross sections at the collision energy 0.1 K. The total number of coupled equations (6) to solve was 1938 for $M=0$. This is 2 times as large as the basis sets used in our previous calculations without hyperfine interactions [27,32].

## III. RESULTS

### A. Potential energy surface for YbF-He

Figure 1 presents the contour plot of the PES for YbF-He. The global minimum of the potential occurs at $R=9.6a_0$ and $\theta=0$ and it is characterized by $D_e=21.88$ cm$^{-1}$. This geometry corresponds to the linear complex in which He is bound to the YbF molecule on the fluorine side. When $\theta=180°$, the attraction is much smaller and the repulsion begins at larger values of $R$. The He atom is repelled by the outer $6s$ orbital and the filled $f$ subshell. The shallow well depth on the Yb side of YbF is of similar magnitude as the interaction between the free Yb atom and He [24]. The data of Ref. [24] show that $R_e$ for Yb-He is around $11-12a_0$ which is where the He-YbF($^2\Sigma$) PES has a saddle point at $\theta=180°$.

### B. YbF in electric and magnetic fields

At zero fields, the ground rotational level $N=0$ of YbF is split by the hyperfine interaction into two states, $F=0$ and $F=1$. The $F=0$ state is lower in energy. Figure 2 shows that magnetic fields split the $F=1$ level into three Zeeman states corresponding to different values of the projections $M_S$ and $M_I$ indicated in the graph. The Zeeman states with $M_S=-\frac{1}{2}$ and $\frac{1}{2}$ correspond to the high-field-seeking and low-field-seeking states, respectively. The fully stretched spin state $|N=0,M_N=0,M_S=\frac{1}{2},M_I=\frac{1}{2}\rangle=|00\frac{1}{2}\frac{1}{2}\rangle$ is denoted by the dashed line in the upper panel of Fig. 2 (for brevity, we omit the labels for the projection quantum numbers). In the following, we will focus on collisions of molecules initially in this state. The transition $|00\frac{1}{2}\frac{1}{2}\rangle\rightarrow|00-\frac{1}{2}-\frac{1}{2}\rangle$ corresponds to the full reorientation of both electronic and nuclear spins. It will be referred to as Zeeman relaxation. The transition to the lowest-energy Zeeman level $|00\frac{1}{2}\frac{1}{2}\rangle\rightarrow|00-\frac{1}{2}\frac{1}{2}\rangle$ approximately conserves the nuclear spin projection so it corresponds to hyperfine relaxation. Both the Zeeman and hyperfine transitions result in reorientation of the electron spin and trap loss and lead to decoherence of the superposition states $\frac{1}{\sqrt{2}}[|F=1,M_F=1\rangle+|F=1,M_F=-1\rangle]$ in the experiments of Hudson *et al.* [3].

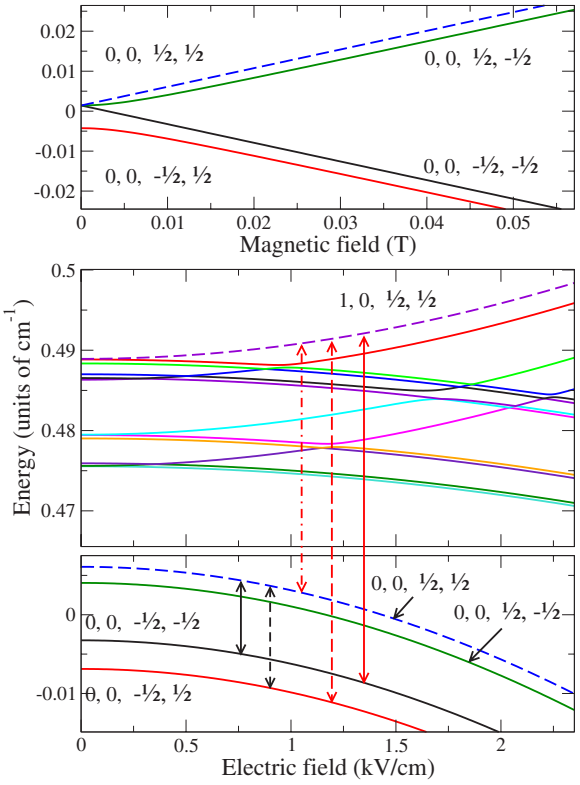


FIG. 2. (Color online) Magnetic levels of the YbF molecule at zero electric field (upper panel); electric field dependence of the molecular states of YbF at a magnetic field of 0.01 T (middle and lower panels). The energy is referred to the ground ro-vibrational state of the molecule at zero fields. The dashed curves in the upper and lower panels denote the low-field seeking state $|00\frac{1}{2}\frac{1}{2}\rangle$, the dashed curve in the middle panel corresponds to the rotationally excited $|10\frac{1}{2}\frac{1}{2}\rangle$ level. Vertical arrows represent the hyperfine relaxation (dashed line), spin relaxation (full line), and spin-conserving rotational relaxation (dashed-dotted line).

The lower panel of Fig. 2 shows the Stark shifts of all the $N=0$ states at a magnetic field of 0.01 T. The energy of the states decreases with increasing electric field and the energy level diagram is qualitatively similar to those for $^2\Sigma$ and $^3\Sigma$ molecules in the absence of the hyperfine interaction [27]. Due to the large electric dipole moment and the small rotational constant of YbF, the Stark shifts are significant already at moderate electric fields, and the states of $N=0$ are strongly mixed with the states of $N=1$ shown in the middle panel of Fig. 2. The first excited rotational level of YbF is split into 12 Zeeman states, and we choose the low-field-seeking state

TABLE I. Coefficients $\alpha$, $\beta$, $\gamma$, $\delta$ in the expansions (9) and (10) of molecular wave functions at an external magnetic field of 0.01 T. The values of the electric field are given in kV/cm. For the functions discussed in the text $\xi_i = \xi_f$, where $\xi$ denotes the coefficients $\alpha$, $\beta$, $\gamma$, $\zeta$.

| Coefficient | $E=0$ | $E=2$ | $E=5$ |
|---|---|---|---|
| $\alpha_i$ | 0.999 | 0.988 | 0.941 |
| $\beta_i$ | 0.0 | 0.153 | 0.336 |
| $\gamma_i$ | 0.0 | $7.0\times10^{-3}$ | $3.8\times10^{-2}$ |
| $\zeta_i$ | $-3.6\times10^{-4}$ | $-3.5\times10^{-4}$ | $-3.2\times10^{-4}$ |

$|10\frac{1}{2}\frac{1}{2}\rangle$ as the initial state for our calculations of rotational relaxation. This state can be trapped in both electrostatic and magnetic traps. Note that the labeling of molecular energy levels in Fig. 2 does not reflect the coupling of the $N=0$ and $N=2$ rotational levels by the hyperfine interaction. The eigenfunction corresponding to the initial low-field-seeking state of $\hat{H}_{\rm mol}$ can be written to first order as

$$\chi_i = \alpha_i|0,0,\tfrac{1}{2},\tfrac{1}{2}\rangle + \beta_i|1,0,\tfrac{1}{2},\tfrac{1}{2}\rangle + \gamma_i|2,0,\tfrac{1}{2},\tfrac{1}{2}\rangle + \zeta_i|2,1,-\tfrac{1}{2},-\tfrac{1}{2}\rangle, \quad (9)$$

where the values of the field-dependent coefficients $\alpha_i$, $\beta_i$, $\gamma_i$, and $\zeta_i$ at $B=0.01$ T are given in Table I. Likewise, the wave function of the final state labeled as $|00-\frac{1}{2}-\frac{1}{2}\rangle$ in Fig. 2 is a superposition of the following terms:

$$\chi_f = \alpha_f|0,0,-\tfrac{1}{2},-\tfrac{1}{2}\rangle + \beta_f|1,0,-\tfrac{1}{2},-\tfrac{1}{2}\rangle + \gamma_f|2,0,-\tfrac{1}{2},-\tfrac{1}{2}\rangle + \zeta_f|2,-2,\tfrac{1}{2},\tfrac{1}{2}\rangle, \quad (10)$$

where the subscript $f$ indicates the final Zeeman state. The small admixture of the $N=2$ state is due to the hyperfine interaction which also mixes the states with different $M_S$ and $M_I$. The magnitude of the mixing coefficient $\zeta$ depends on the energy splitting between the $N=0$ and $N=2$ levels. The hyperfine interaction in $^2\Sigma$ molecules thus plays a role similar to the spin-spin interaction in $^3\Sigma$ molecules [27,33]. Since electric fields couple only the adjacent rotational states (for example, $N=0$ and $N=1$), the coefficients $\zeta_i$ and $\zeta_f$ in Eqs. (9) and (10) do not vary strongly with the electric field. The coefficients $\gamma_i$ and $\gamma_f$ of Table I increase with increasing electric field.

### C. Magnetic field dependence of Zeeman relaxation rates

The cross sections for Zeeman and hyperfine relaxation at a collision energy of 0.1 K are displayed in Fig. 3 as functions of the magnetic field strength. At zero electric field, the initial decrease of the cross sections is followed by a broad maximum around 0.25 T. Nonzero electric fields (Fig. 3, middle and lower panels) induce resonances in the magnetic-field dependence of the cross sections. The first resonance at $E=10$ kV/cm and $B\sim0.11$ T enhances the Zeeman relaxation cross sections by almost three orders of magnitude. Increasing the electric field up to 20 kV/cm changes the positions of the resonances and modifies their widths. As explained below, the resonances in Fig. 3 are Feshbach resonances.

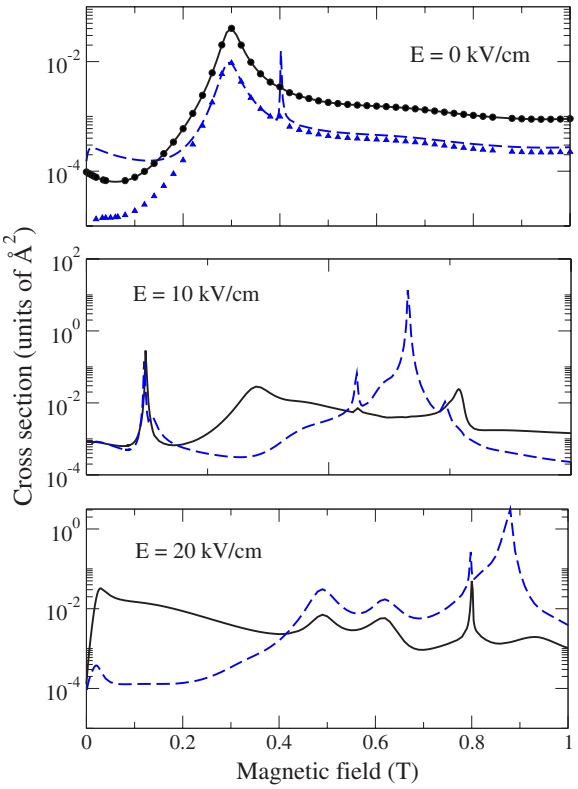


FIG. 3. (Color online) Magnetic field dependence of the Zeeman (full line) and hyperfine relaxation (dashed line) cross sections at zero electric field (upper panel), $E=10$ kV/cm (middle panel), and $E=20$ kV/cm (lower panel). The symbols in the upper panel are the results of the calculations without the spin-rotation interaction. The collision energy is 0.1 K.

To understand the role of the spin-rotation interaction in YbF-He collisions, we have repeated the calculations with zero spin-rotation interaction constant $\gamma$. The upper panel of Fig. 3 shows that the Zeeman relaxation cross sections do not change whereas the hyperfine relaxation is suppressed by a factor of 20 at low magnetic fields. This suggests that the hyperfine relaxation occurs through coupling between the ground and rotationally excited levels (induced by the interaction potential) and the reorientation of molecular spin due to the spin-rotation interaction. This mechanism was first suggested by Krems *et al.* [34] for spin depolarization of $^2\Sigma$ molecules.

The Zeeman transitions from the fully stretched state to the lower magnetic states of the $F=1$ triplet appear to follow a different trend. In the absence of the hyperfine interaction, the projection of the nuclear spin on the magnetic field axis must be conserved and the Zeeman transitions cannot occur. We have verified this in a calculation with the constants $b$ and $c$ both set to zero. As shown in the upper panel of Fig. 3, the spin-rotation interaction does not assist the Zeeman relaxation and we conclude that the Zeeman relaxation cross sections are entirely determined by the hyperfine interaction. The Zeeman transitions are mediated by the anisotropy of the atom-molecule interaction potential through (1) direct cou-

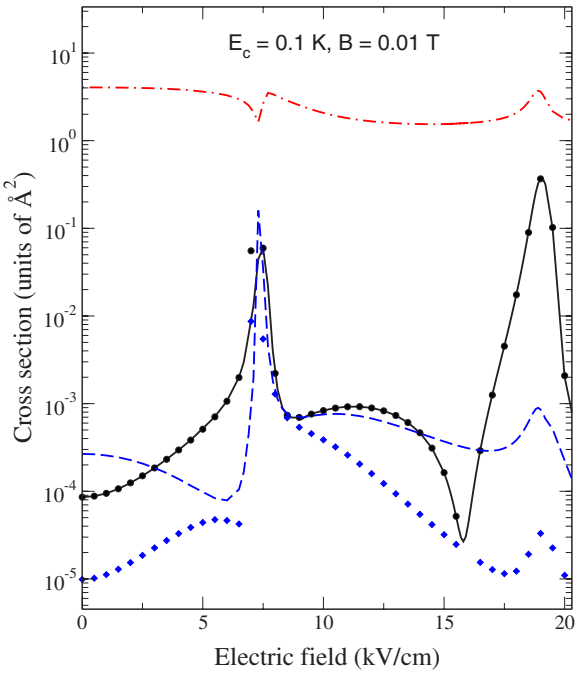


FIG. 4. (Color online) Electric field dependence of nuclear spin-changing (full line) and nuclear-spin conserving (dashed line) Zeeman cross sections at a magnetic field of 0.01 T and a collision energy of 0.1 K. The uppermost curve is the elastic scattering cross section divided by $10^3$ to fit the scale of the graph, symbols denote the results of the calculations without the spin-rotation interaction.

plings due to the admixture of the $N=2$ states in the rotationally ground state of the molecule [cf. Eq. (9) and Ref. [33]] and (2) indirect couplings involving a sequence of virtual transitions to rotationally excited states and the interaction between the rotational angular momentum of the molecule and the spins in the tensor product $[\hat{I}\otimes\hat{S}]^{(2)}$. To elucidate which couplings are more important we repeated the calculations without the $N=2$ level. This resulted in an increase of the Zeeman relaxation cross sections. Omitting the $N=2$ level from the basis set changes the structure of the diatomic molecule to a great extent so this test cannot be regarded as quantitatively conclusive. However, it indicates that the indirect couplings in collisions of YbF with He are significant and may be stronger than the direct couplings.

### D. Electric field dependence of YbF-He interactions

Figure 4 shows the dependence of the Zeeman and hyperfine relaxation cross sections on the electric field at a magnetic field of 0.01 T and a collision energy of 0.1 K typical of buffer-gas loading experiments [9]. The range of electric fields chosen corresponds to the EDM search experiments of Hinds and co-workers [3]. The cross sections vary by three orders of magnitude near the resonances at 7 and 18 kV/cm. The hyperfine relaxation is suppressed at low electric fields. A similar behavior of the Zeeman relaxation cross sections with increasing electric field has been observed previously for CaD($^2\Sigma$)-He collisions [27,32]. This again emphasizes the similarity between the hyperfine relaxation and the spin

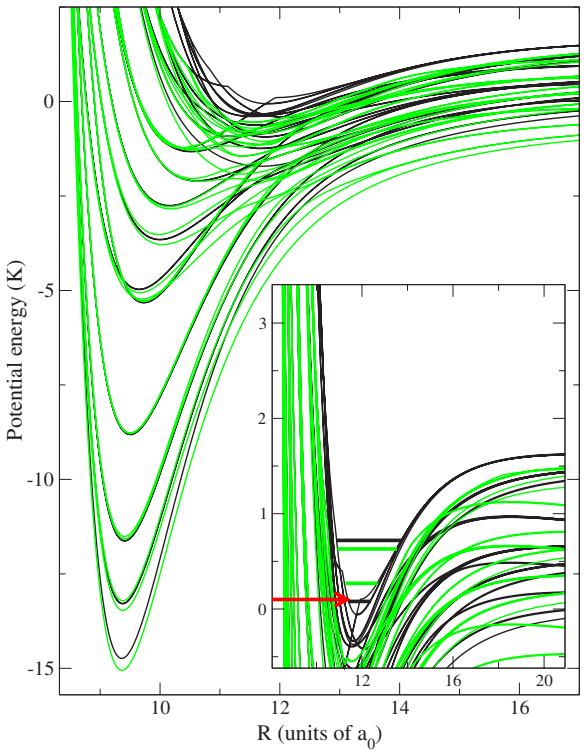


FIG. 5. (Color online) Adiabatic potential curves as functions of the center-of-mass YbF-He separation $R$. The black curves correspond to zero electric fields, the curves are calculated at $E=10$ kV/cm. The inset shows the bound levels of the YbF···He complex: the black bars at zero electric field, the bars at $E=10$ kV/cm. Horizontal arrow in the inset marks the collision energy (the zero of energy corresponds to the separated YbF and He fragments). The magnetic field is 0.01 T.

flipping transitions in $^2\Sigma$ molecules with zero nuclear spin discussed in Sec. III A. The probability of the Zeeman transition $|00\frac{1}{2}\frac{1}{2}\rangle\rightarrow|00-\frac{1}{2}-\frac{1}{2}\rangle$ increases with increasing electric field.

Bohn and co-workers [17] observed resonance structures in ultracold collisions of OH molecules in the presence of an electric field and ascribed them to threshold resonances in incoming collision channels. To verify that the peaks in Fig. 4 are due to scattering resonances, we diagonalized the matrix of the Hamiltonian (1) at fixed atom-diatom distances $R$ in the basis of four rotational functions ($N_{\max}=3$) and four partial waves ($\ell_{\max}=3$). To reduce computational effort, we omitted the hyperfine interaction from Eq. (1) which resulted in a total of 84 eigenstates for $M=1/2$. Figure 5 shows the eigenvalues of the Hamiltonian as functions of the YbF-He separation at a magnetic field of 0.01 T.

Electric fields modify the adiabatic potential curves and induce additional interactions between the rotational levels. As a result, some zero-field crossings shown in Fig. 5 are transformed into avoided crossings. We have computed the quasibound levels of the YbF···He van der Waals complex in a magnetic field using the Fourier grid Hamiltonian method [35]. The resonance states shown in Fig. 5 shift as the electric field increases. Feshbach resonances arise when the positions of these levels match the collision energy (marked by

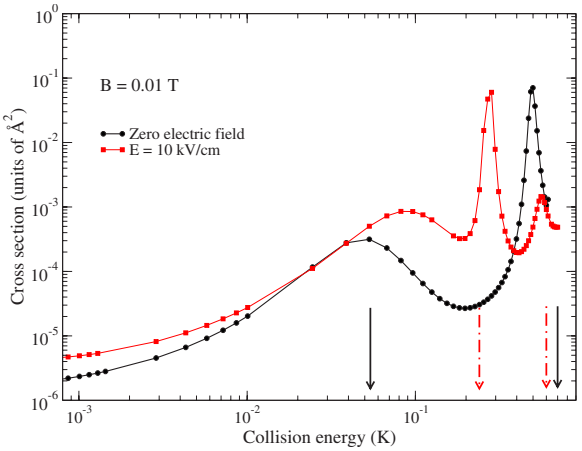


FIG. 6. (Color online) Collision energy dependence of cross sections for the nuclear spin-changing $|00\frac{1}{2}\frac{1}{2}\rangle \rightarrow |00-\frac{1}{2}-\frac{1}{2}\rangle$ or Zeeman transition. The electric field values are zero (circles) and 10 kV/cm (squares), and the magnetic field is 0.01 T. Vertical arrows mark the position of the bound levels from Fig. 5 at zero electric field (full arrows) and $E=10$ kV/cm (dashed-dotted arrows).

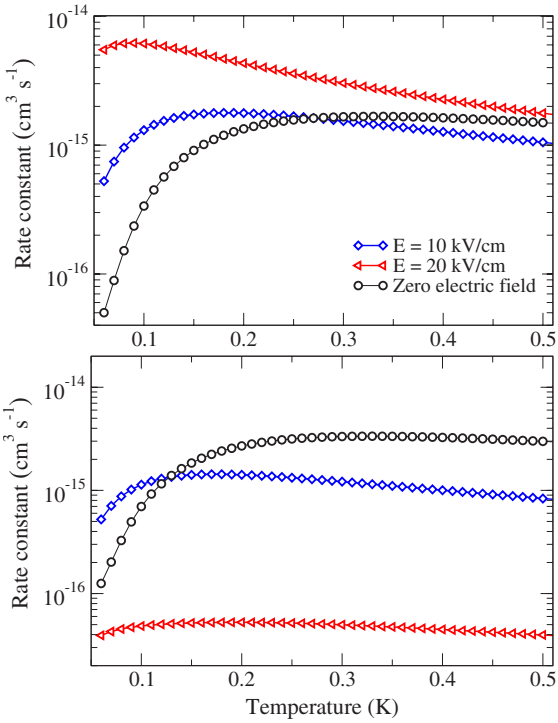


FIG. 7. (Color online) Rate constants for the nuclear spin-changing or Zeeman (upper panel) and nuclear spin-conserving or hyperfine (lower panel) transitions as functions of temperature at a magnetic field of 0.01 T. The electric field is zero (circles), 10 kV/cm (diamonds), and 20 kV/cm (triangles).

the arrow in Fig. 5). The elastic cross section decreases near the first resonance at 7.5 kV/cm. The ratio of the cross sections for elastic scattering and Zeeman relaxation remains large, $1.7\times10^4$ (see Fig. 8 below). At zero electric field, this ratio exceeds $1.5\times10^6$ which suggests that YbF molecules can be good candidates for cryogenic cooling experiments in a buffer gas of He [7,9]. Interestingly, the Feshbach resonances shown in Figs. 4 and 5 have not been observed in low-energy collisions of CaH and NH molecules [32–34] in ground rotational states. The rotational level splittings in these molecules are large compared to the strength of their interactions with He, which results in larger splittings of the adiabatic curves (Fig. 5) and "isolation" of rotationally ground state from the excited states.

Figure 6 demonstrates the Feshbach resonances in the dependence of Zeeman cross sections on the collision energy $\epsilon$. At zero electric field, there are two broad resonances at $\epsilon=0.07$ and 0.74 K, while at $E=10$ kV/cm the resonances get closer to each other, and so do the quasibound levels indicated by the arrows in Fig. 5. At lower collision energies, the cross sections at $E=10$ kV/cm are larger than at zero electric field, in agreement with our earlier results for $^2\Sigma$ molecules [32].

To elucidate the possibility of cryogenic cooling and magnetic trapping of YbF, we have calculated the cross sections for Zeeman and hyperfine relaxation as well as elastic scattering, on a dense grid of 160 collision energies from 0.007 to 0.7 K to obtain thermal rate constants. Because of the $N=1$ thresholds, the energy dependence of the cross sections in this interval is complicated. We approximated the calculated cross sections by cubic spline functions and truncated the integration over the collision energy at 0.7 K. The resulting rate constants are accurate to within the factor of 5. The rate constants for the Zeeman relaxation as functions of temperature are shown in Fig. 7. Electric fields shift Feshbach resonances and increase rate constants for the nuclear spin-changing transition. On the other hand, the nuclear spin-conserving transition is suppressed by electric fields at 0.1 K. At higher temperatures, the resonant enhancement of the cross section leads to an increase of the rate. Figure 7 shows that the rate constants for the Zeeman relaxation show different behavior under the influence of the electric field. This suggests that electric fields can be used for selective suppression or enhancement of the spin relaxation pathways. For example, the Feshbach resonance shown in Fig. 6 moves to the left with increasing electric field. This leads to an enhancement of the rate constants for Zeeman relaxation at $E=20$ kV/cm shown in the upper panel of Fig. 7.

The ratio of elastic and Zeeman relaxation rate constants is shown in Fig. 8 as a function of the temperature. The ratio varies moderately over the temperature range 0.06–0.6 K. Electric fields suppress inelastic transitions in the hyperfine channel (lower panel) which is compensated by the increasing rate of the Zeeman relaxation (upper panel).

### E. Rotational relaxation of YbF

Figure 9 shows the dependence of the cross section for the transitions from the highest low-field-seeking state in the rotationally excited $N=1$ manifold of levels (see Fig. 2) to the four states of the lowest rotational level. The nuclear spin-conserving transitions are suppressed by the electric field similarly to how rotational relaxation is suppressed in $^2\Sigma$ molecules [27]. As we have shown in Sec. III C, these transitions are driven by the spin-rotation interaction. Electric

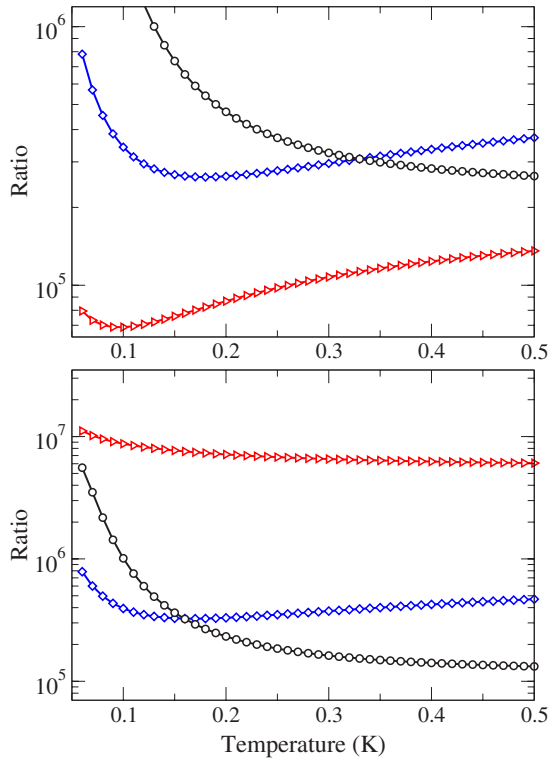


FIG. 8. (Color online) The ratio of the rate constants for elastic scattering and Zeeman (upper panel) and hyperfine (lower panel) relaxation as functions of temperature at a magnetic field of 0.01 T. The electric field is zero (circles), 10 kV/cm (diamonds), and 20 kV/cm (triangles).

fields split the levels corresponding to the different $|M_N|$ and reduce the strength of the effective spin-rotation interaction thereby inhibiting spin relaxation.

On the contrary, the nuclear spin-changing transition $|10\frac{1}{2}\frac{1}{2}\rangle \rightarrow |00-\frac{1}{2}-\frac{1}{2}\rangle$ is only weakly affected by electric

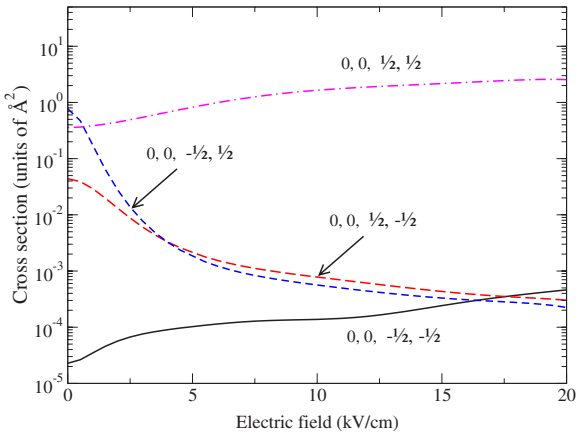


FIG. 9. (Color online) Cross sections for rotational relaxation from the low-field-seeking state $|10\frac{1}{2}\frac{1}{2}\rangle$ as functions of the electric field at a magnetic field of 0.01 T and a collision energy of 0.1 K. The dominant components of the final states are $|00-\frac{1}{2}-\frac{1}{2}\rangle$ (full line), $|00-\frac{1}{2}\frac{1}{2}\rangle$ (short dashed line), $|00\frac{1}{2}-\frac{1}{2}\rangle$ (long dashed line), and $|00\frac{1}{2}\frac{1}{2}\rangle$ (dashed-dotted line). The cross section for the electron and nuclear spin-conserving transition $|10\frac{1}{2}\frac{1}{2}\rangle \rightarrow |00\frac{1}{2}\frac{1}{2}\rangle$ is divided by 100 to fit the scale of the graph.

TABLE II. Electric field dependence of rate constants for transitions from the $|10\frac{1}{2}\frac{1}{2}\rangle$ state of YbF in collisions with He at a magnetic field of 0.01 T and temperature of 0.5 K.

| Electric field (kV/cm) | Final state $(N, M_N, M_S, M_I)$ | Rate constant, cm$^3$/s |
|---|---|---|
| 0 | $\|00-\frac{1}{2}-\frac{1}{2}\rangle$ | $7.1\times10^{-17}$ |
| | $\|00-\frac{1}{2}\frac{1}{2}\rangle$ | $4.7\times10^{-14}$ |
| | $\|00\frac{1}{2}-\frac{1}{2}\rangle$ | $7.6\times10^{-13}$ |
| | $\|00\frac{1}{2}\frac{1}{2}\rangle$ | $3.5\times10^{-11}$ |
| | $\|1-1-\frac{1}{2}-\frac{1}{2}\rangle$ | $7.9\times10^{-17}$ |
| | $\|1-1-\frac{1}{2}\frac{1}{2}\rangle$ | $1.8\times10^{-14}$ |
| | $\|1-1\frac{1}{2}-\frac{1}{2}\rangle$ | $2.7\times10^{-13}$ |
| | $\|1-1\frac{1}{2}\frac{1}{2}\rangle$ | $2.5\times10^{-11}$ |
| | $\|10-\frac{1}{2}-\frac{1}{2}\rangle$ | $2.2\times10^{-15}$ |
| | $\|10-\frac{1}{2}\frac{1}{2}\rangle$ | $3.3\times10^{-14}$ |
| | $\|10\frac{1}{2}-\frac{1}{2}\rangle$ | $9.6\times10^{-13}$ |
| | $\|10\frac{1}{2}\frac{1}{2}\rangle$ | $3.9\times10^{-10}$ |
| | $\|11-\frac{1}{2}-\frac{1}{2}\rangle$ | $9.7\times10^{-14}$ |
| | $\|11-\frac{1}{2}\frac{1}{2}\rangle$ | $4.5\times10^{-14}$ |
| | $\|11\frac{1}{2}-\frac{1}{2}\rangle$ | $8.3\times10^{-13}$ |
| | $\|11\frac{1}{2}\frac{1}{2}\rangle$ | $2.6\times10^{-11}$ |
| 10 | $\|00-\frac{1}{2}-\frac{1}{2}\rangle$ | $3.3\times10^{-17}$ |
| | $\|00-\frac{1}{2}\frac{1}{2}\rangle$ | $4.8\times10^{-16}$ |
| | $\|00\frac{1}{2}-\frac{1}{2}\rangle$ | $2.8\times10^{-16}$ |
| | $\|00\frac{1}{2}\frac{1}{2}\rangle$ | $4.2\times10^{-11}$ |
| | $\|1-1-\frac{1}{2}-\frac{1}{2}\rangle$ | $1.0\times10^{-16}$ |
| | $\|1-1-\frac{1}{2}\frac{1}{2}\rangle$ | $2.8\times10^{-16}$ |
| | $\|1-1\frac{1}{2}-\frac{1}{2}\rangle$ | $8.7\times10^{-17}$ |
| | $\|1-1\frac{1}{2}\frac{1}{2}\rangle$ | $2.8\times10^{-11}$ |
| | $\|10-\frac{1}{2}-\frac{1}{2}\rangle$ | $1.0\times10^{-16}$ |
| | $\|10-\frac{1}{2}\frac{1}{2}\rangle$ | $4.6\times10^{-16}$ |
| | $\|10\frac{1}{2}-\frac{1}{2}\rangle$ | $1.4\times10^{-16}$ |
| | $\|10\frac{1}{2}\frac{1}{2}\rangle$ | $3.9\times10^{-10}$ |
| | $\|11-\frac{1}{2}-\frac{1}{2}\rangle$ | $1.0\times10^{-13}$ |
| | $\|11-\frac{1}{2}\frac{1}{2}\rangle$ | $4.8\times10^{-16}$ |
| | $\|11\frac{1}{2}-\frac{1}{2}\rangle$ | $2.9\times10^{-16}$ |
| | $\|11\frac{1}{2}\frac{1}{2}\rangle$ | $2.8\times10^{-11}$ |

fields. As shown in Sec. III B, this process is determined by the hyperfine interaction which depends on the splitting between the $N=2$ and $N=0$ levels. Electric fields do not couple these states so they do not affect nuclear spin-changing transitions to a great extent. The results shown in Fig. 9 are consistent with our earlier study of rotational relaxation of $^2\Sigma$ and $^3\Sigma$ molecules [27]. They show that heavy molecules can follow two distinct rotational relaxation pathways that share common features with similar processes in molecules with zero nuclear spin: (1) the nuclear spin-conserving relaxation pathway driven by the spin-rotation couplings like the spin relaxation in $^2\Sigma$ molecules, and (2) the nuclear spin-changing pathway mediated by the hyperfine interaction

similar to the spin-spin interaction in $^3\Sigma$ molecules.

The rate constants for the transitions from the highest low-field-seeking state $|10\frac{1}{2}\frac{1}{2}\rangle$ are given in Table II. Electric fields suppress spin-changing transitions, slightly increase the propensity for spin-conserving rotational relaxation, and leave elastic scattering cross sections unaltered. The results presented in Table II suggest that magnetic trapping of YbF molecules in the $|10\frac{1}{2}\frac{1}{2}\rangle$ state may be facilitated by applying electric fields on the order of 10 kV/cm. Comparison with Fig. 7 reveals that the rates for spin relaxation of the $N=0$ state are larger at $E=10$ kV/cm. The Feshbach resonances (Figs. 5 and 6) enhance spin relaxation of YbF molecules in the ground rotational state. Because of the larger splitting between the $N=1$ and $N=2$ levels, the Feshbach resonances for collisions of YbF molecules in the rotationally excited $N=1$ state occur at lower collision energy and they do not affect rate constants at $T=0.5$ K.

## IV. CONCLUSION

We have presented a quantum mechanical study of collisions between YbF molecules and He atoms in electric and magnetic fields at temperatures below 1 K. YbF is a molecule with small rotational constant and strong hyperfine interaction. We have shown that the simultaneous electron and nuclear spin depolarization in collisions of YbF in the rotationally ground state occurs through coupling to rotationally excited states and the action of the hyperfine interaction. The electron spin-depolarization conserving the nuclear spin projection is determined by the spin-rotation interaction, in agreement with earlier studies of collisions of $^2\Sigma$ molecules without the hyperfine effects [34]. We have found that the overall rate of magnetic relaxation of rotationally ground-state YbF molecules in a gas of He is very small. At temperatures between 0.05 K and 0.6 K, the ratio of the rate constants for elastic YbF-He collisions and inelastic Zeeman and hyperfine relaxation is larger than $10^4$. Apparently, the anisotropy of the YbF-He interaction is so small that it does not allow for efficient spin-depolarization of YbF, despite the small rotational constant of the molecule. These results suggest that molecules with small rotational constants may be amenable to buffer gas loading experiments using He gas.

We have shown that the dynamics of YbF-He collisions at temperatures below 1 K can be effectively manipulated by electric fields. The cross sections for elastic scattering, Zeeman and hyperfine relaxation as well as rotationally inelastic transitions can be extremely sensitive to the magnitude of an applied electric field near electric field-induced Feshbach resonances. The results shown in Fig. 4 suggest that the EDM experiments with magnetically trapped YbF molecules in a buffer gas of He should be performed at electric fields far detuned from Feshbach resonances to prevent spin decoherence and trap loss. In addition, external electric fields decrease the coupling between the rotational angular momentum of the molecule and the spin so the transitions determined by the spin-rotation interaction can be significantly suppressed by electric fields of $\sim 10$ kV/cm.

We have found that spin-relaxation of rotationally excited molecules at $T=0.5$ K is much slower than the Zeeman and hyperfine transitions in the ground rotational states in the presence of electric fields. This happens because the electric-field-induced Feshbach resonances that enhance the spin relaxation occur at much lower collision energies when the molecule is in the $N=1$ state. The resonances should disappear if the molecule is excited to higher rotational states.

Our study elucidates the propensities for collisional depolarization of the nuclear and electron spins in heavy molecules with small rotational constants. Collisional spin-depolarization of molecules leads to quantum decoherence of superposition spin states in molecular interferometry experiments and determines the stability of molecular ensembles in a magnetic trap. The complexity of diatomic molecules allows for new degrees of freedom in experiments with cold molecular gases. The results presented here improve our understanding of molecular interactions in external fields and may help with the choice of systems for future cold molecule experiments.

## ACKNOWLEDGMENTS

The authors thank Andrea Simoni for providing a program for bound state calculations. The work of two of the authors (R.V.K. and T.V.T.) was supported by the Natural Sciences and Engineering Research Council (NSERC) of Canada and the Killam Trusts. One of the authors (J.K.) was supported by NSF Grant No. CHE04-0413743, and one of the authors (L.R.) was supported by NSF Grant No. CHE-0414241.

[1] M. G. Kozlov and L. N. Labzowsky, J. Phys. B **28**, 1933 (1995).
[2] M. G. Kozlov and D. DeMille, Phys. Rev. Lett. **89**, 133001 (2002).
[3] J. J. Hudson, B. E. Sauer, M. R. Tarbutt, and E. A. Hinds, Phys. Rev. Lett. **89**, 023003 (2002).
[4] The most recent attempt to measure the EDM with YbF molecules is described in B. E. Sauer, H. T. Ashworth, J. J. Hudson, M. R. Tarbutt, and E. A. Hinds, e-print physics/0611155.
[5] D. Egorov, J. D. Weinstein, D. Patterson, B. Friedrich, and J. M. Doyle, Phys. Rev. A **63**, 030501(R) (2001).
[6] E. Hinds, Phys. Scr. **T70**, 34 (1997).
[7] M. R. Tarbutt, H. L. Bethlem, J. J. Hudson, V. L. Ryabov, V. A. Ryzhov, B. E. Sauer, G. Meijer, and E. A. Hinds, Phys. Rev. Lett. **92**, 173002 (2004).
[8] S. E. Maxwell, N. Brahms, R. deCarvalho, J. S. Helton, S. Nguyen, D. Patterson, J. M. Doyle, D. R. Glenn, J. Petricka, and D. DeMille, Phys. Rev. Lett. **95**, 173201 (2005).
[9] J. M. Doyle, B. Friedrich, J. Kim, and D. Patterson, Phys. Rev. A **52**, R2515 (1995).
[10] R. V. Krems and A. Dalgarno, J. Chem. Phys. **120**, 2296 (2004).

[11] K. Maussang, D. Egorov, J. S. Helton, S. V. Nguyen, and J. M. Doyle, Phys. Rev. Lett. **94**, 123002 (2005).
[12] A. Volpi and J. L. Bohn, Phys. Rev. A **65**, 052712 (2002).
[13] B. E. Sauer, J. Wang, and E. A. Hinds, J. Chem. Phys. **105**, 7412 (1996).
[14] M. H. Alexander and P. J. Dagdigian, J. Chem. Phys. **83**, 2191 (1985).
[15] F. Daniel, M.-L. Dubernet, and M. Meuwly, J. Chem. Phys. **121**, 4540 (2004).
[16] J. Stutzki and G. Winnewisser, Astron. Astrophys. **144**, 1 (1985).
[17] A. V. Avdeenkov and J. L. Bohn, Phys. Rev. A **66**, 052718 (2002).
[18] A. V. Avdeenkov, M. Kajita, and J. L. Bohn, Phys. Rev. A **73**, 022707 (2006).
[19] C. Ticknor and J. L. Bohn, Phys. Rev. A **71**, 022709 (2005).
[20] M. Lara, J. L. Bohn, D. Potter, P. Soldan, and J. M. Hutson, Phys. Rev. Lett. **97**, 183201 (2006).
[21] MOLPRO is a package of *ab initio* programs written by H.-J. Werner and P. J. Knowles, with contributions from R. D. Amos, A. Berning, D. L. Cooper, M. J. O. Deegan, A. J. Dobbyn, F. Eckert, C. Hampel, T. Leininger, R. Lindh, A. W. Lloyd, W. Meyer, M. E. Mura, A. Nicklaß, P. Palmieri, K. Peterson, R. Pitzer, P. Pulay, G. Rauhut, M. Schütz, H. Stoll, A. J. Stone, and T. Thorsteinsson.
[22] S. F. Boys and F. Bernardi, Mol. Phys. **19**, 553 (1970).
[23] X. Cao and M. Dolg, J. Chem. Phys. **115**, 7348 (2001).
[24] A. A. Buchachenko, M. M. Szczęśniak, and G. Chałasiński, J. Chem. Phys. **124**, 114301 (2006).
[25] T. H. Dunning, J. Chem. Phys. **90**, 1007 (1989).
[26] R. A. Kendall, G. Chałasiński, J. Kłos, R. Bukowski, M. W. Severson, M. M. Szczęśniak, and S. M. Cybulski, J. Chem. Phys. **108**, 3235 (1998).
[27] T. V. Tscherbul and R. V. Krems, J. Chem. Phys. **125**, 194311 (2006).
[28] R. N. Zare, *Angular Momentum* (Wiley, New York, 1988).
[29] M. Mizushima, *The Theory of Rotating Diatomic Molecules* (Wiley, New York, 1975); K.-P. Huber and G. Herzberg, *Constants of Diatomic Molecules* (Van Nostrand Reinhold, New York, 1979).
[30] A. V. Titov, N. S. Mosyagin, and V. F. Ezhov, Phys. Rev. Lett. **77**, 5346 (1996).
[31] M. G. Kozlov and V. F. Ezhov, Phys. Rev. A **49**, 4502 (1994).
[32] T. V. Tscherbul and R. V. Krems, Phys. Rev. Lett. **97**, 083201 (2006).
[33] R. V. Krems, H. R. Sadeghpour, A. Dalgarno, D. Zgid, J. Kłos, and G. Chałasiński, Phys. Rev. A **68**, 051401(R) (2003).
[34] R. V. Krems, A. Dalgarno, N. Balakrishnan, and G. C. Groenenboom, Phys. Rev. A **67**, 060703(R) (2003).
[35] D. T. Colbert and W. H. Miller, J. Chem. Phys. **96**, 1982 (1992).